ESA Contract Report

SMOS ESL contract 4000130567/20/I-BG

Contract Report to the European Space Agency

Annual SMOS brightness temperature monitoring report - 2020/21

Authors: Pete Weston and Patricia de Rosnay
Contract officer: Raffaele Crapolicchio

November 2021

Series: ECMWF - ESA Contract Report

A full list of ECMWF Publications can be found on our web site under:

http://www.ecmwf.int/publications/

European Centre for Medium Range Weather Forecasts
Shinfield Park, Reading, RG2 9AX, England

Abbreviations

BUFR ..... Binary Universal Form for the Representation of meteorological data
CMEM ..... Community Microwave Emissivity Modelling platform
ECMWF ..... European Centre for Medium-range Weather Forecasts
ESA ..... European Space Agency
IFS ..... Integrated Forecast System
NRT ..... Near Real Time
NWP ..... Numerical Weather Prediction
RFI ..... Radio Frequency Interference
SMAP ..... Soil Moisture Active Passive
SMOS ..... Soil Moisture and Ocean Salinity
Tb ..... Brightness Temperature

1. Introduction

This document provides an annual summary of the performance of the European Space Agency (ESA) Soil Moisture and Ocean Salinity (SMOS) brightness temperature (Tb) monitoring run routinely at the European Centre for Medium-range Weather Forecasts (ECMWF). The period covered is September 2020 to August 2021. Several different monitoring plots are presented, and notable features are described in detail. Also, potential improvements to the monitoring system are proposed.

2. Annual SMOS monitoring results

Routine operational monitoring of SMOS observations from the NRT BUFR product is performed at ECMWF. The SMOS measured brightness temperatures are compared to short-term numerical weather prediction (NWP) forecasts transformed into brightness temperatures using the Community Microwave Emissivity Model (CMEM). The differences between these two quantities are known as background departures and statistics of these background departures are accumulated and plotted routinely.

The samples used to produce the plots can be filtered by area, including global, Northern and Southern Hemispheres, as well as loose definitions of the continents: Europe (120°W-120°E, 35°N-77.5°N), Asia (0°W-120°W, 40°N-82.5°N), North America (120°E-0°E, 20°N-77.5°N), South America (120°E-0°E, 40°S-17.5°N) and Australia (0°E-120°W, 47.5°S-7.5°S). This section focuses on global statistics.

Also, the plots are produced separately for data:

- Over sea or over land
- With different incidence angles: 30°, 40° or 50°
- With different polarisations: H (XX) or V (YY) at the SMOS antenna reference frame

A selection of different options for surface type, incidence angles and polarisations are presented, and the full set of plots are available via FTP at ftp://dpgswebserver-2.smos.eo.esa.int/SMOS_ESL2021/Task-5/Annual_Monitoring/2021/All_plots.zip).

A thorough introduction to the monitoring system can be found in Weston and de Rosnay (2020) and examples of the plots produced can be seen at https://www.ecmwf.int/en/forecasts/quality-our-forecasts/monitoring/smos-monitoring. In this section each of the different types of plots produced as part of the SMOS monitoring system are presented and any notable features are highlighted to be investigated in more detail in the following sections.

2.1. Time series

Statistics are plotted as lines against time on the x-axis for the full twelve-month period with statistics accumulated in 12 hour chunks. The statistics plotted are mean and standard deviation of background departures, the mean observed and background brightness temperatures and number of observations. These plots allow global trends and jumps in the statistics to be identified.

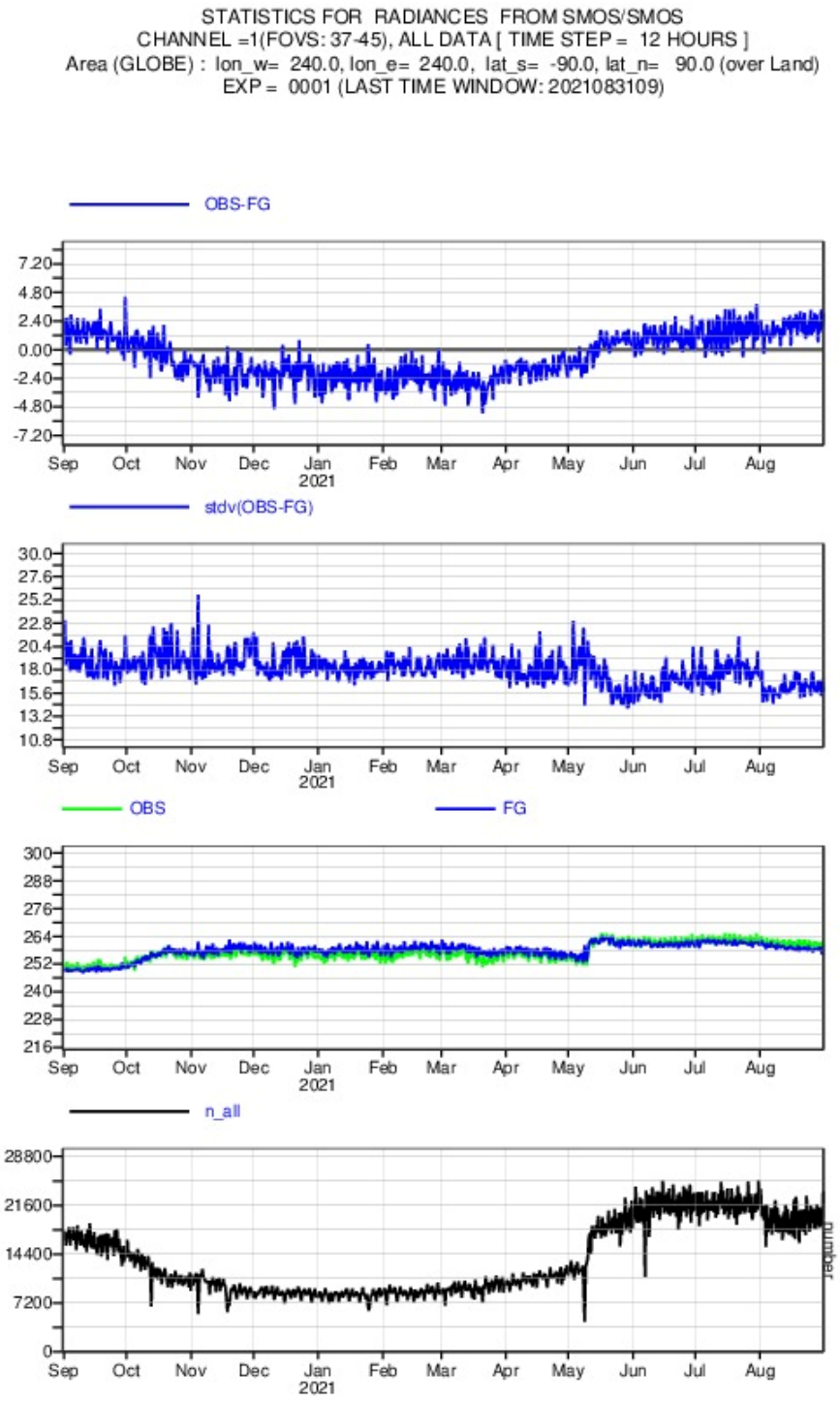

Figure 1: Time series of mean background departures (upper panel), standard deviation of background departures (2nd panel), mean observed and background values (3rd panel) and number of observations (lower panel). Statistics are accumulated for SMOS observations over land at 40° incidence angle, H polarisation and cover 1st September 2020 to 31st August 2021

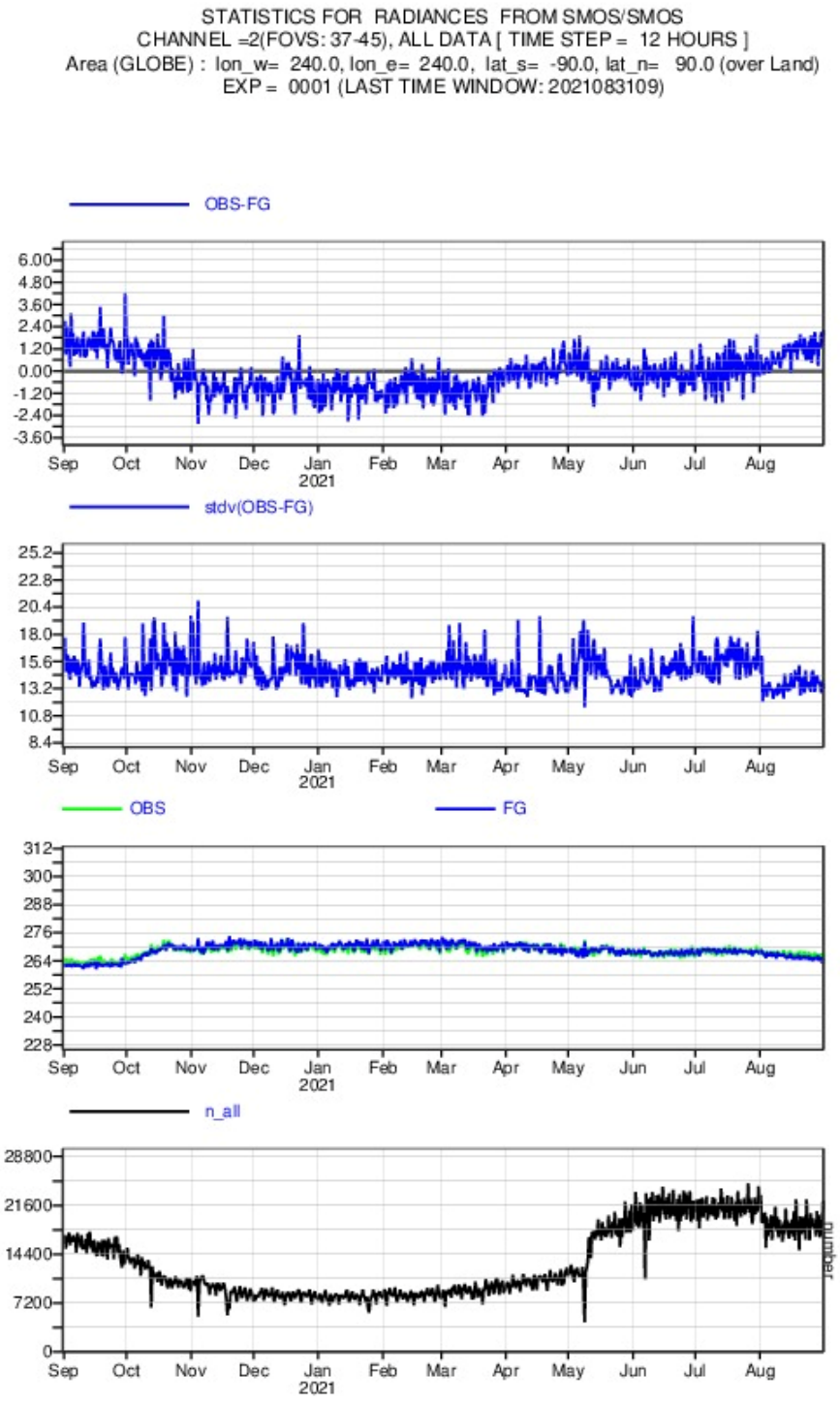

Figure 2: As figure 1 but for SMOS observations with V polarisation

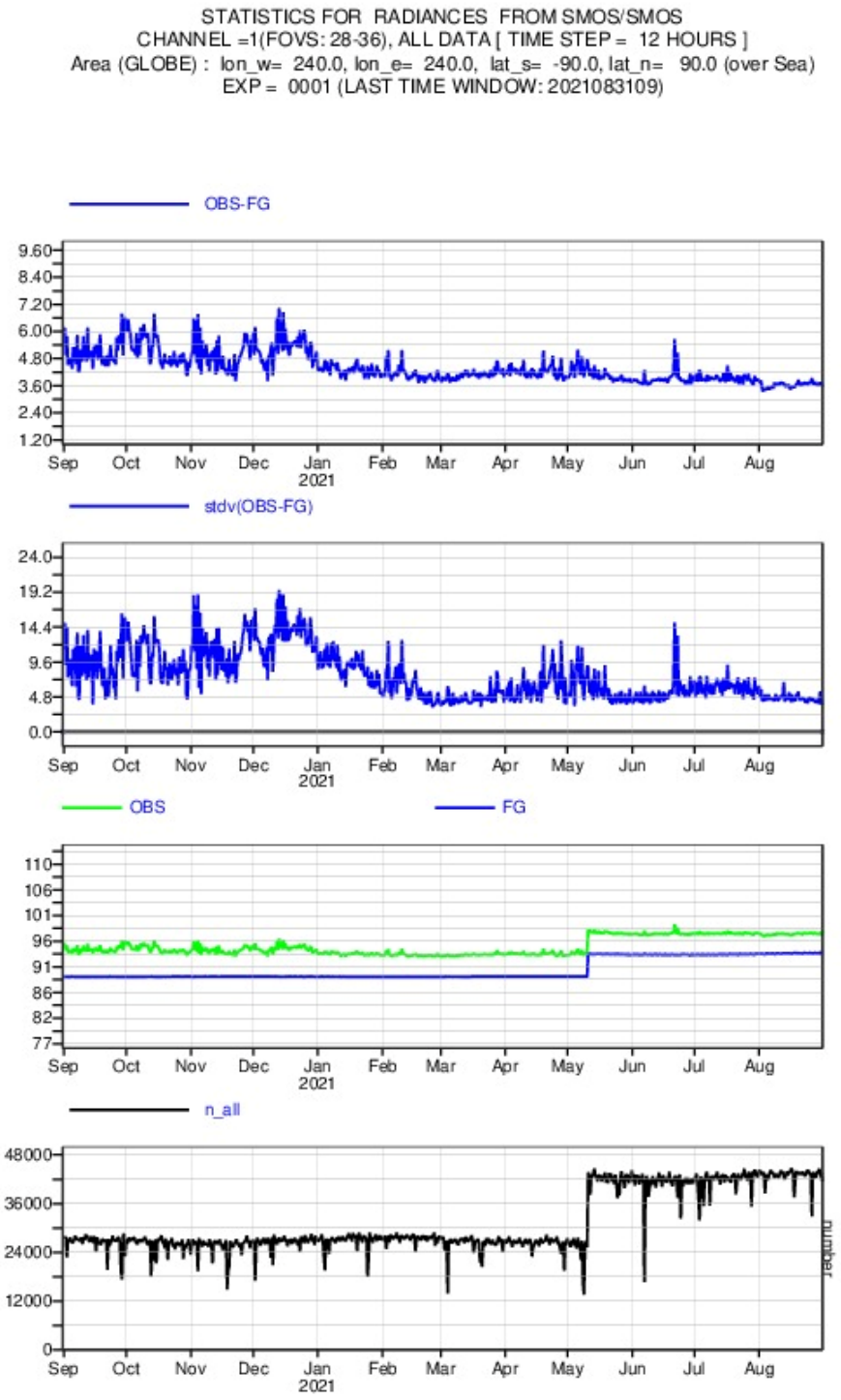

Figure 3: As figure 1 but statistics are accumulated for SMOS observations over ocean at 30° incidence angle, H polarisation and cover 1st September 2020 to 31st August 2021

Figures 1 and 2 show that the background departure statistics over land are generally very stable over the year. The mean background departures mostly vary between ±5K for H polarisations and ±3K for V polarisations with only very occasional global mean values outside of this range. The standard

deviation of background departures have slightly more day-to-day variability but generally stay close to a value of 20K for H polarisations and 15K for V polarisations. The apparent slightly better performance of the V polarisations over the H polarisations could be due to an instrument effect but it could also be due to differing performance of the CMEM observation operator used to convert the model soil moisture to brightness temperature. It should be noted that the first guess departures presented here do not have a bias correction applied and the statistics are consistent with those found between 2010 and 2016 without bias correction in de Rosnay et al (2020). The largest variation is seen in the number of observations monitored. Between September 2020 and December 2020 there is a significant reduction of almost 50% in the number of observations monitored. This is due to the Northern hemisphere winter and many observations over Northern hemisphere land surfaces being screened out due to frozen soil and snow. At the same time there is a corresponding negative shift in the mean background departures due to the different sampling as described in Weston & de Rosnay (2021a). Between March 2021 and May 2021 this trend is reversed as the Northern hemisphere summer starts and the land thaws out. On 11th May 2021 there is a sudden increase in the number of SMOS observations monitored. This coincides with the implementation of the latest ECMWF model cycle, 47r2, and corresponding changes to the quality control procedures applied to the SMOS data for which the monitoring statistics are calculated. See section 3.1 for more details. On the 2nd August 2021 there is a smaller step change in the number of observations and some of the background departure statistics. This coincides with the switch to the newly processed v724 SMOS level 1 brightness temperatures, see section 3.2 for more details.

Figure 3 shows that there is larger annual variability in the background departure statistics over ocean than over land, particularly between September 2020 and January 2021. The increases in both mean and standard deviation of background departures coincide with the Antarctic sea-ice melting period and are caused by sub-optimal frozen surface screening which means that observations over sea-ice with much larger background departures contaminate the global sample. As part of the upgrade implemented on 11th May 2021 the sea-ice screening was improved which results in a much more stable evolution of the background departures during the Arctic sea-ice melting period from May to August 2021. Also, the mean background and observation values increase by approximately 5K due to this change. See section 3.1 for more details. The number of observations between September 2020 and May 2021 is much more stable over ocean than over land. A similar sudden increase on 11th May 2021 is seen over ocean as over land, again corresponding to the quality control change (section 3.1).

2.2. Hovmöller plots

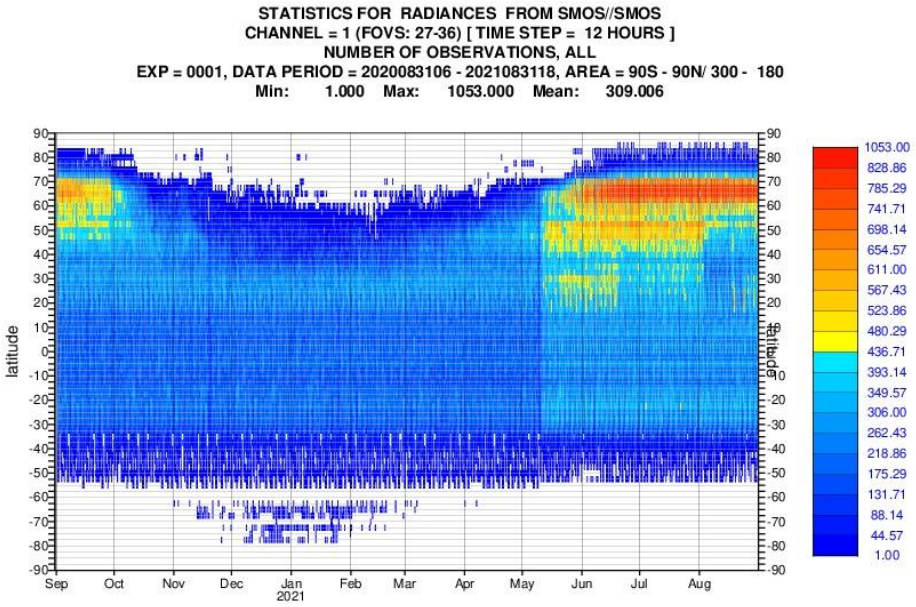

Figure 4: Hovmöller plot showing the number of SMOS observations monitored over land at 30° incidence angle, H polarisation covering 1st September 2020 to 31st August 2021

Statistics presented in this section are plotted as a heat map (Hovmöller plots) with time on the x-axis and latitude on the y- axis for the twelve-month period with statistics accumulated in 2.5° latitude bins and 12 hour chunks. The statistics plotted are mean and standard deviation of background departure, mean and standard deviation of observed value and number of observations. These plots allow local trends and jumps in the statistics to be identified. Figure 4 shows that the number of SMOS observations monitored over land varies significantly over the year. Between September and December 2020, the number of observations significantly reduces between 40°N and 80°N. As seen in the time series plots this is due to the Northern hemisphere winter and many observations at these latitudes being screened out due to frozen surfaces. The effect is enhanced at these latitudes because SMOS is in a polar orbit and the swathes start to overlap near the poles therefore there are more observations in these areas than in the tropics. The opposite effect can also be seen between April 2021 and June 2021 as the Northern hemisphere summer begins. The number of observations over the tropics and Southern hemisphere varies far less over the year. The same sharp increase in observations can be seen from 11th May 2021 due to the quality control change. Also, there is a marked reduction in the number of observations between 30°N and 55°N from 2nd August 2021. Again, this coincides with the change to the v724 SMOS level 1 brightness temperatures processor, see section 3.2 for more details.

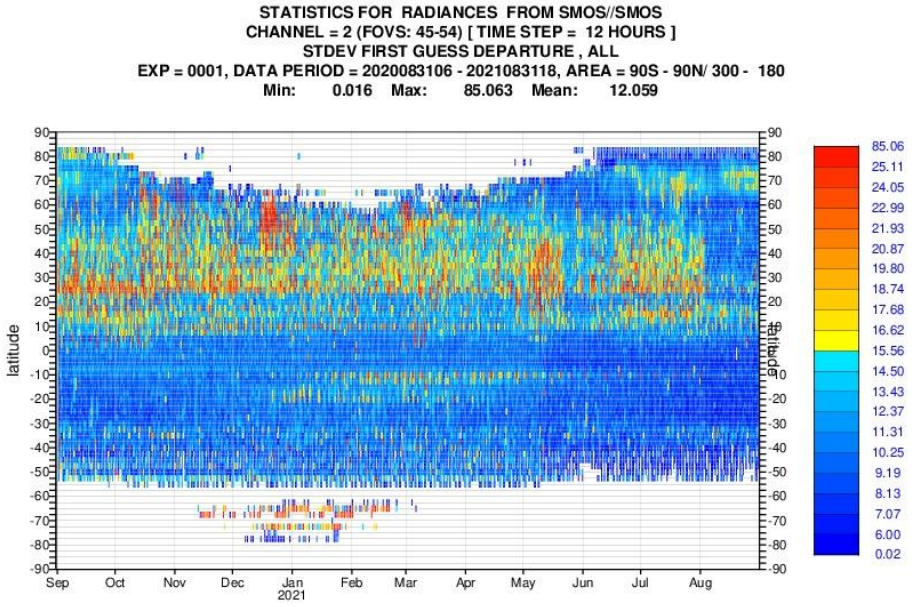

Figure 5: Hovmöller plot showing SMOS first guess departure standard deviation monitored over land at 50° incidence angle, V polarisation covering 1st September 2020 to 31st August 2021

Figure 5 shows that from the 11th May 2021 onwards there is a small decrease in the standard deviation of background departures over land, particularly visible in the tropics and Southern hemisphere. This is related to the quality control change. The effect is less marked in the Northern hemisphere due to the higher prevalence of RFI which causes the larger standard deviation of background departures which are present before and after 11th May because the RFI screening was not changed. However, from the 2nd August there is a reduction in the standard deviation of background departures particularly between 30°N and 55°N. This is the same area where there is a reduction in number of observations monitored (figure 4) and suggests that the newly re-processed v724 SMOS L1 brightness temperatures have enhanced RFI screening which is helping to remove more RFI affected observations than the screening in the previous v620 SMOS L1 product. See section 3.2 for more details.

2.3. Maps

Label	Start and end dates	Description
Period 1	1st September 2020 to 30th April 2021	Before the quality control change
Period 2	1st June 2021 to 31st July 2021	After the quality control change
Period 3	1st August 2021 to 31st August 2021	After the switch to v724 SMOS L1 product

Table 1: Periods for which statistics are accumulated for the gridded maps

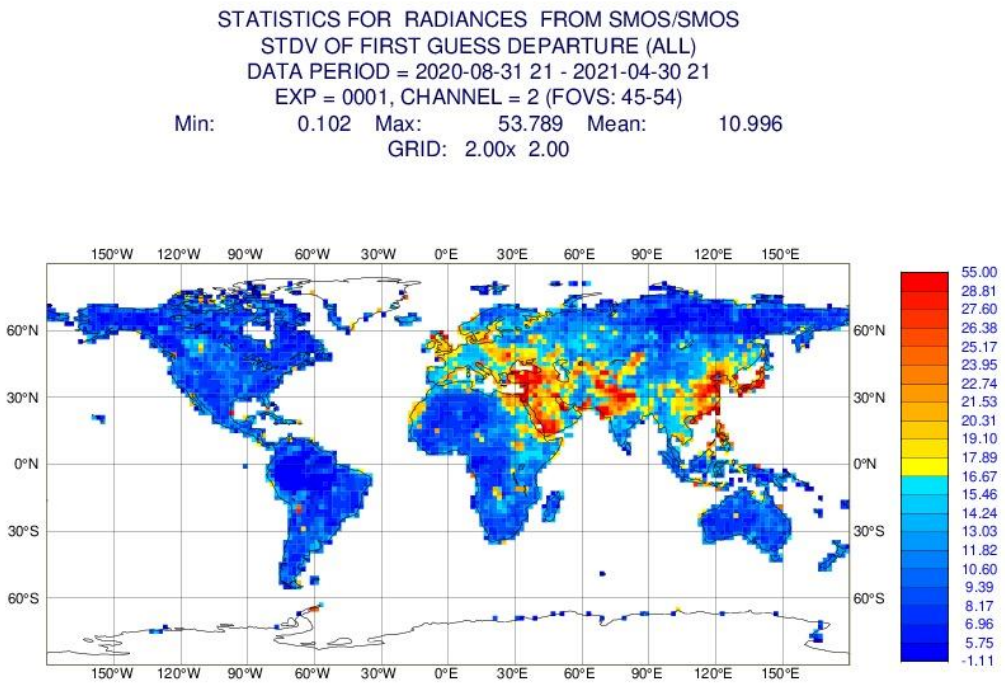

Figure 6: Map plot showing the standard deviation of SMOS background departures over land at 50° incidence angle, V polarisation covering period 1 (see table 1)

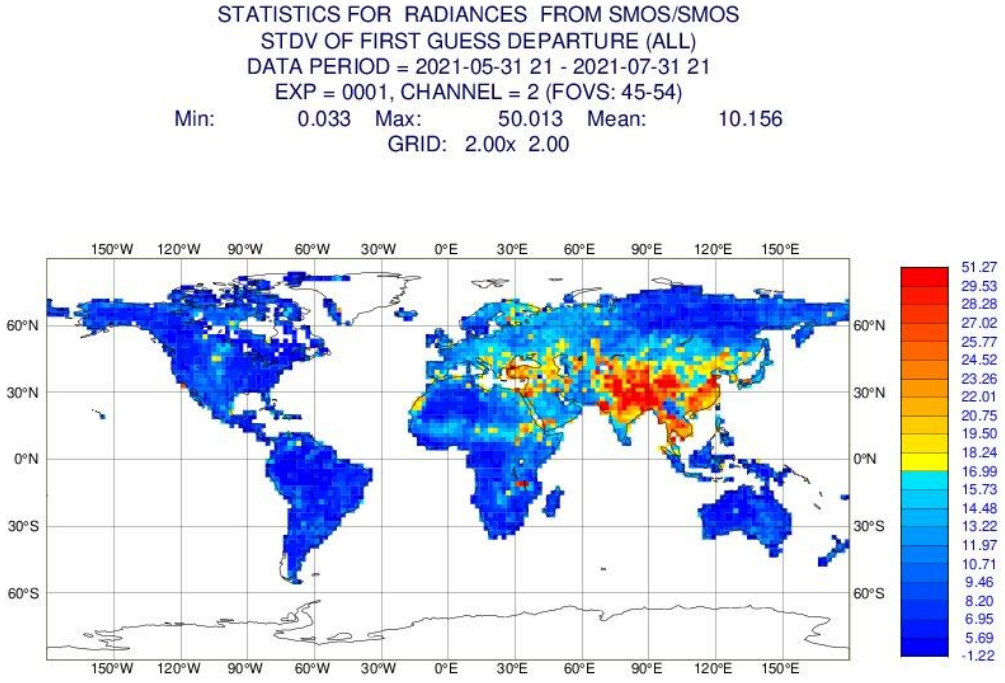

Figure 7: As figure 6 but with statistics covering period 2 (see table 1)

Due to the shifts in statistics from May 11th 2021 and 2nd August 2021 the statistics for the gridded maps are accumulated in 3 separate periods described in table 1.

Figures 6 and 7 shows largest background departures over the Middle East, central and Eastern Asia, and to a lesser extent Europe. This is caused by RFI in those regions and the differences in the worst affected areas in figure 6 and 7 indicates that RFI sources vary in strength and location over time. The signal from the RFI completely swamps any signal coming from changes in soil moisture which means it is very important to correctly screen out RFI. Figures 9, 10 and 11 show that the effect of RFI also extends over ocean around the coasts surrounding Europe, the Middle East, and Eastern Asia too.

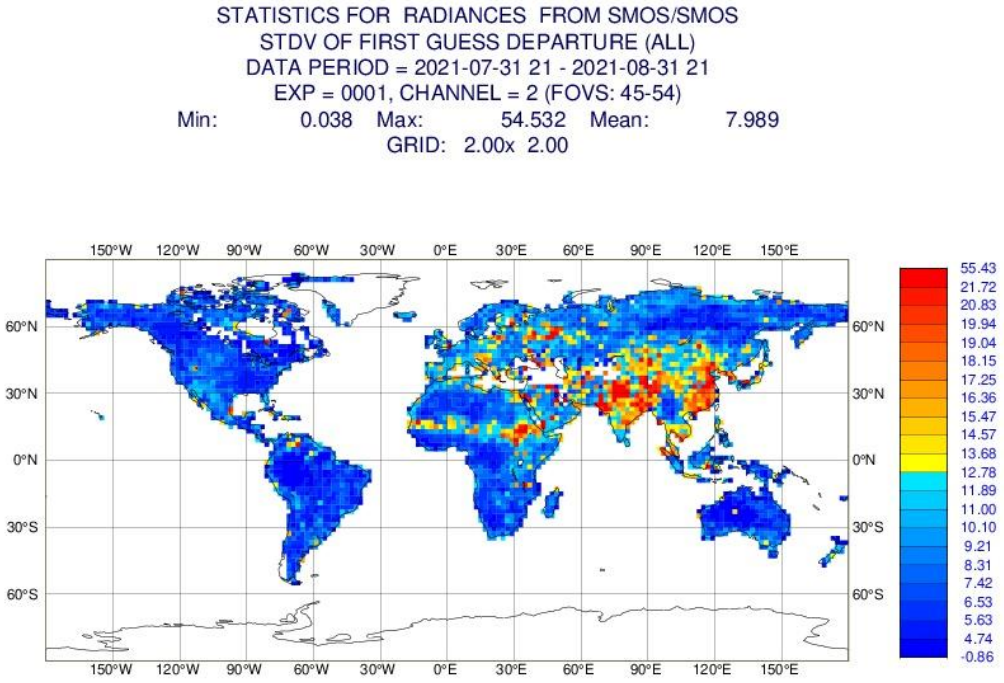

Figure 8: As figure 6 but with statistics covering period 3 (see table 1)

Figure 8 still shows large areas of background departures over the same regions but the background departures are slightly smaller (lower values in the colour scale) and the areas affected slightly reduced in size. Also, there are blank areas over the middle East indicating no valid observations over this region in this period. The mean value of the standard deviation of background departures reduces from 10.156K in period 2 to 7.989K in period 3. This provides further evidence that the RFI screening in the new v724 SMOS L1 Tbs is improved compared to the previous version operational before August 2021.

Some of the quality control differences implemented on 11th May 2021 can be seen when comparing figures 6 and 7. In particular, there are fewer coloured pixels around the coasts, islands and inland lakes (e.g. over Svalbard). This is due to enhanced coastal screening as part of the suite of quality control changes.

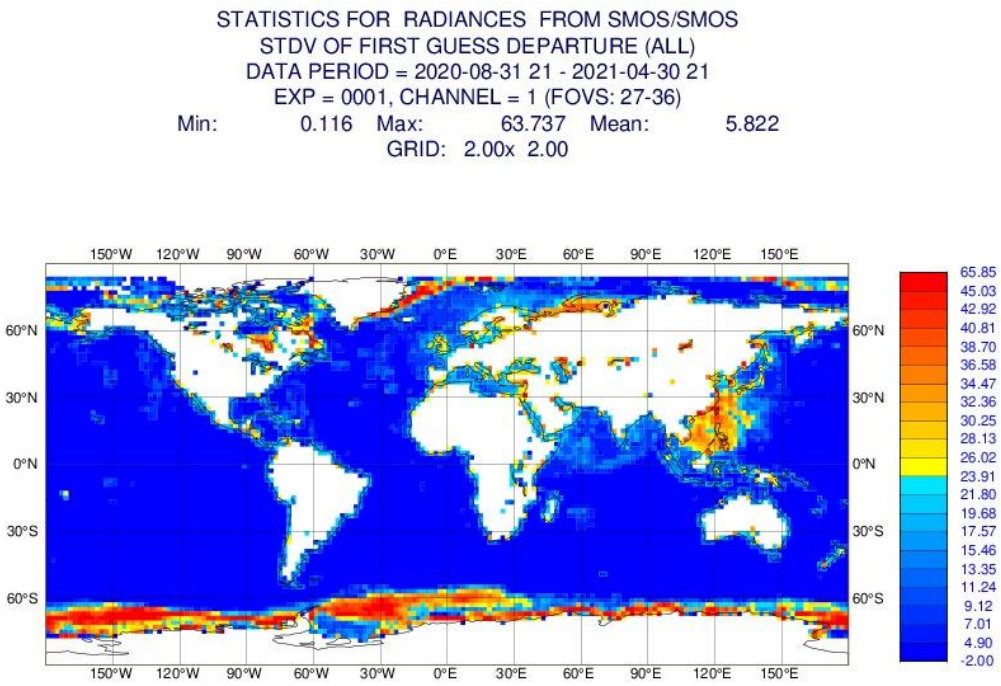

Figure 9: Map plot showing the standard deviation of SMOS background departures over ocean at 30° incidence angle, H polarisation covering period 1 (see table 1)

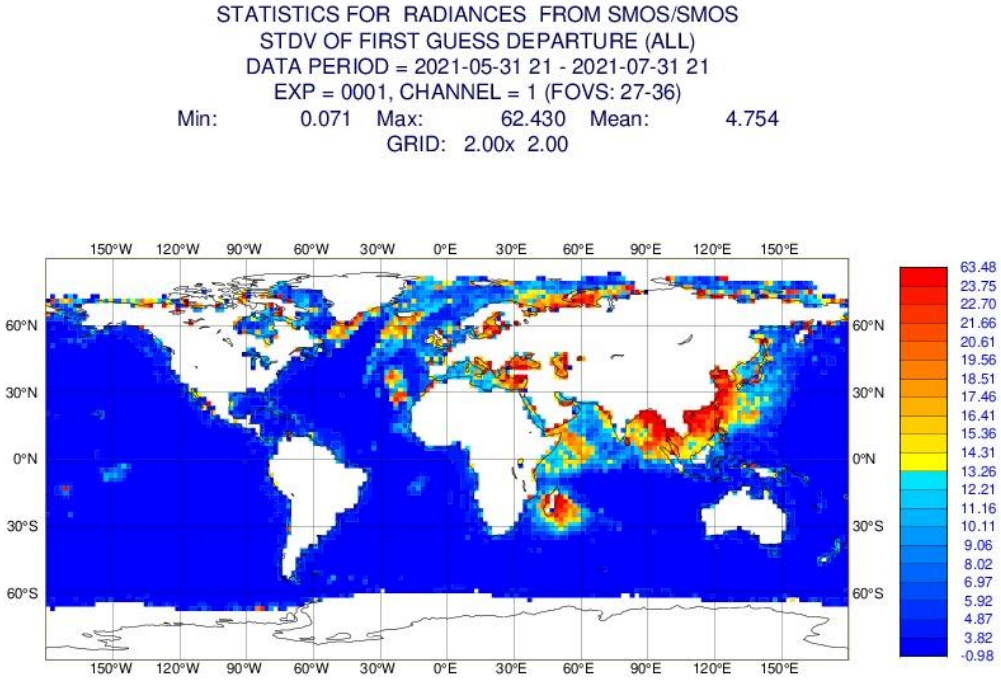

Figure 10: As figure 9 but with statistics covering period 2 (see table 1)

Figure 9 shows areas of increased background departures over the Northern and Southern polar regions. This is related to the sub-optimal sea-ice screening. Figure 10 shows that these areas have been screened out and this is due to the additional sea-ice screening implemented from 11th May 2021 onwards. Figure 10 also shows a reduction or removal of large departures around some coastal regions (e.g. Hudson Bay) and inland lakes (e.g. lake Baikal in Eastern Russia) corresponding to the enhance coastal screening as mentioned previously. The remaining areas of large background departures in figure 10 are due to RFI contamination. Away from these RFI affected areas there is very little variation in background departures due to lower Tb variations over ocean which are mostly caused by temperature variations. In addition, the observation operator CMEM treats the sea surfaces like lake surfaces. Hence, there is currently no variation in simulated brightness temperature from waves or surface wind-speed as there will be in the observed brightness temperatures.

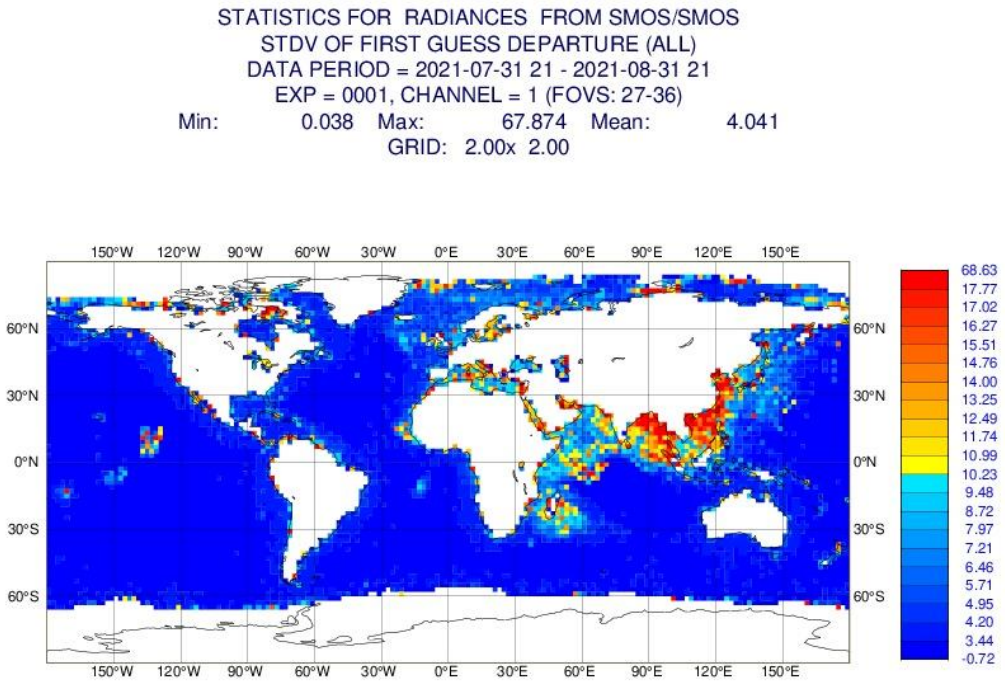

Figure 11: As figure 9 but with statistics covering period 3 (see table 1)

Comparing figures 10 and 11 shows that the areas affected by RFI are reduced in period 3 compared to period 2 (note the colour scale change) especially over the Black and Caspian Seas, North coast of Russia, Baltic Sea and surrounding Madagascar. Some of these changes may be due to temporal variability in the RFI sources but the number of observations in these regions is also reduced with the move to the v724 SMOS L1 product suggesting enhanced RFI screening.

2.4. Scatter

Statistics are accumulated from 1st September 2020 to 31st August 2021 and plotted as a 2-dimensional histogram with incidence angle on the x-axis and background departure on the y-axis. These plots allow the distributions of background departures at different incidence angles to be analysed.

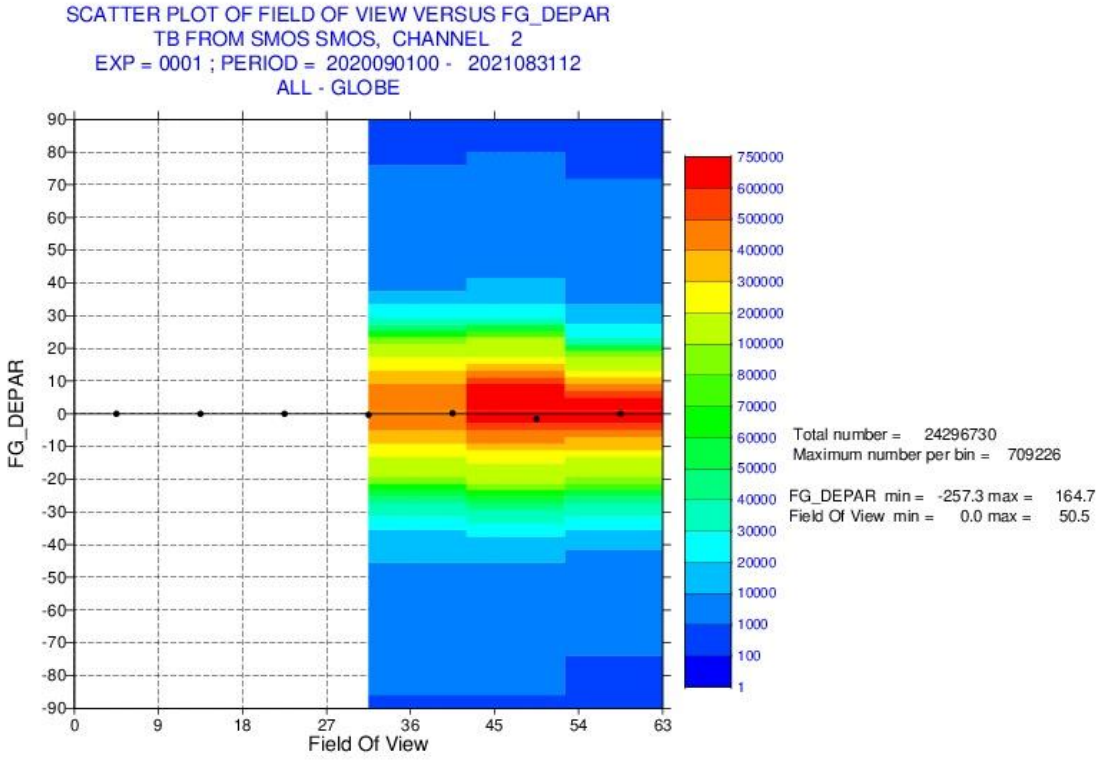

Figure 12: Scatter plot showing a 2D-histogram of SMOS background departures over land for different incidence angle bins, V polarization covering 1st September 2020 to 31st August. The black dots represent the mean background departure for each incidence angle bin

Figure 12 shows that the distribution of background departures is centred close to zero for all incidence angle bins. It also shows that the histograms are close to symmetric, which can be seen by looking at the number of observations in the background departure bins with a similar magnitude but opposite signs. The global mean background departures for each incidence angle bin are also close to zero although there are significant regional biases, see section 4.1.

3. Notable features in 2020/21

This section describes notable features which are visible in the monitoring plots for September 2020 to August 2021.

3.1. Change of quality control procedures with 47r2 implementation on 11th May 2021

As seen clearly in figures 1 to 4 there was a significant increase in the number of SMOS observations monitored from 11th May 2021 and other changes to the background departure statistics covered

throughout section 2. This corresponds to the implementation of ECMWF cycle 47r2 which included changes to the quality control procedures, many of which were described in the annual SMOS Tb monitoring report 2019/20 (Weston & de Rosnay, 2021a). The main changes which were implemented are summarised in table 2 and for more details see appendix A and Weston & de Rosnay, 2021b.

Quality control change	Qualitative effect on monitoring statistics
Inclusion of extended alias-free zone observations	A significant increase in the number of observations monitored over ocean and land at incidence angles of 30 and 40 degrees with a very small effect on background departure statistics
Enhanced sea-ice screening	A reduction in the number of observations monitored over ocean at high latitudes and a large reduction in both mean and standard deviation of background departures
Coastal screening	A reduction in the number of observations monitored over ocean and land around coasts, islands and inland lakes and a small reduction in the mean and standard deviation of background departures

Table 2: Description of the quality control changes operationally implemented from 11th May 2021

Figure 13 shows a snapshot comparison of the SMOS data coverage before and after the changes where each of the three changes from table 2 are illustrated. The wider swaths in the lower panel indicate the additional extended alias-free zone observations. The removal of the large positive departures just North of Antarctica between 120°W and 90°W illustrates the improved sea-ice screening. Finally, the removal of large departures around all of the coastlines and inland lakes (e.g. West coast of South America and Baltic Sea) illustrates the additional coastal screening.

Table 3 shows that for incidence angles of 30 and 40 degrees there is an increase in the number of SMOS observations monitored. This is due to the inclusion of the extended alias-free zone observations. For incidence angles of 50 degrees the number of observations decreases because there are very few observations at this incidence angle in the extended alias-free zone so the other quality control changes, which generally reduce the number of observations, dominate.

Over land, there is a reduction in the standard deviation of background departures for H polarisation mainly due to the additional coastal screening. For V polarisation there is a slight reduction at 30 degrees incidence angle, a slight increase at 40 degree incidence angle and a more significant reduction at 50 degrees incidence angle. The coastal screening is causing the reduction and the extended alias-free zone observations cause a slight increase. The balance between these effects is dependent on the number of extended alias-free zone observations at the different incidence angles.

Over ocean, there are large reductions in both the mean and standard deviation of background departures which is mainly due to the enhanced sea-ice screening although the coastal screening also has a small impact.

Overall, figure 13 and table 3 show a significant improvement to the background departure statistics and more SMOS observations being monitored in 47r2 which is operational from 11th May 2021 onwards.

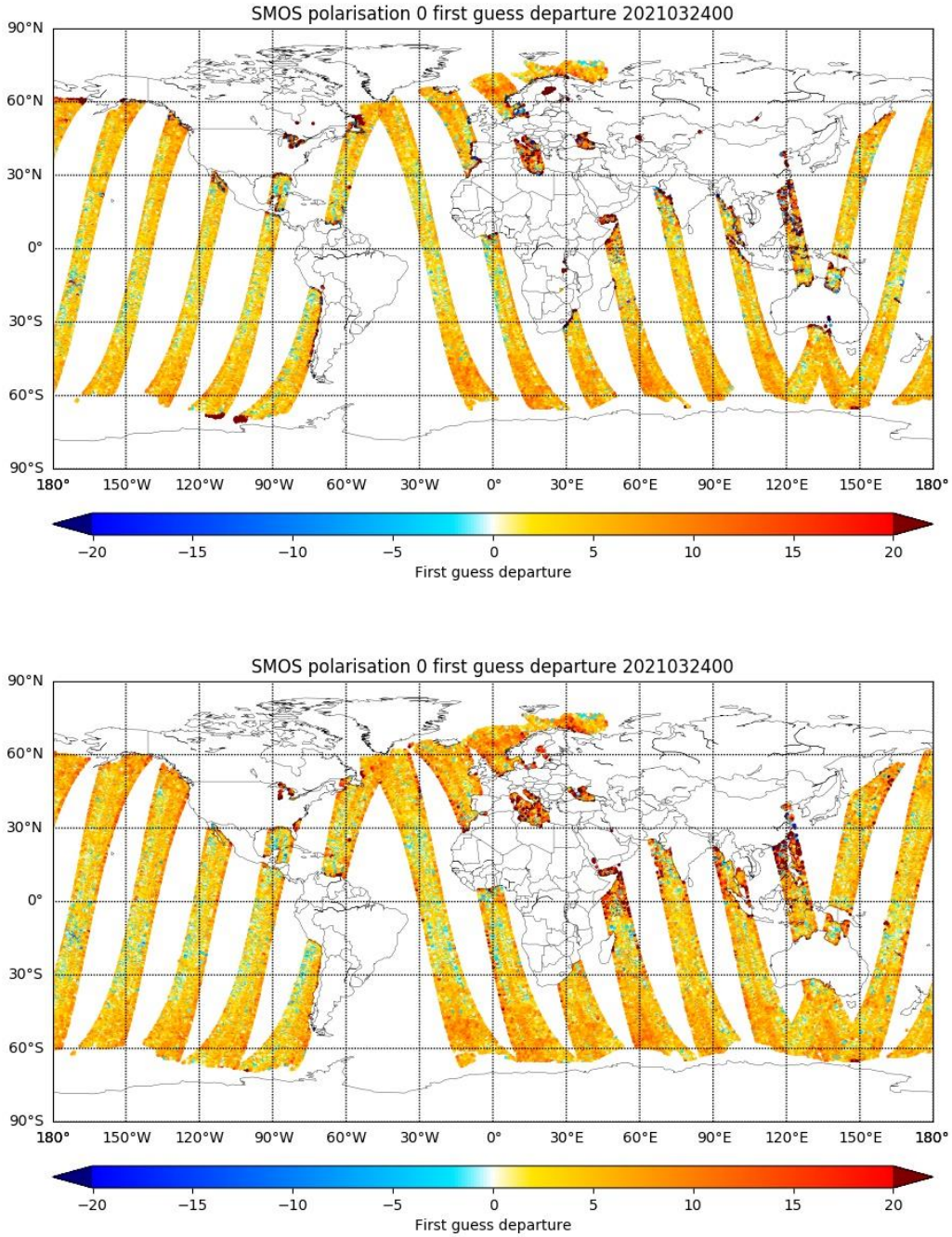

Figure 13: Snapshot maps showing SMOS background departures over ocean at H polarisation from 21:00 UTC on 23rd March 2021 to 09:00 UTC on 24th March 2021 for all observations passing quality control for 47r1 (operational before 11th May 2021, upper panel) and 47r2 (operational after 11th May 2021, lower panel)

Configuration			47r1			47r2		
Sfc	**Pol**	**Inc ang**	**Count**	**Mean bg depar (K)**	**Stdev bg depar (K)**	**Count**	**Mean bg depar (K)**	**Stdev bg depar (K)**
Land	H	30	759512	-0.591	16.911	998443	0.556	15.628
	H	40	1069018	-0.388	17.313	1372871	0.613	16.07
	H	50	1046639	-3.094	18.642	875275	-3.13	17.972
	V	30	731612	-0.498	15.032	959740	-1.335	14.913
	V	40	1021701	-0.185	13.965	1311434	-0.658	14.167
	V	50	988449	-2.465	12.991	819610	-2.08	11.973
Ocean	H	30	1923448	13.465	30.845	2633329	3.733	5.372
	H	40	2820451	14.493	31.492	3714355	4.911	5.468
	H	50	2804935	15.841	31.348	2477014	5.963	5.15
	V	30	1918390	11.15	29.72	2654302	1.349	5.293
	V	40	2812843	11.768	28.823	3734606	2.686	5.447
	V	50	2797051	11.296	26.257	2469972	2.821	5.124

Table 3: Global statistics for different surface types, polarisations and incidence angles for the SMOS observations passing quality control in experiments testing the quality control changes implemented on 11th May 2021. Data is accumulated between 16th June 2019 and 15th July 2019

3.2. Switch to v724 SMOS L1 Tbs from 2nd August 2021

On the 2nd August 2021 ECMWF started receiving v724 SMOS L1 Tbs instead of the previously received v620 product. As seen in a number of figures in section 2 this resulted in a significant change in the background departure statistics which appeared to be mainly as a result of improvements to RFI screening in the new product. In this section a more systematic comparison between the v620 and v724 products is performed. In the absence of parallel acquisition of the two products the comparison will be done on datasets from two different periods. The v620 data used are from 1st July to 31st July 2021 and the v724 data used are from 2nd August to 31st August 2021. One downside to comparing data from different dates is that the RFI sources and geophysical signals that SMOS measures can vary in strength and location for the different periods. The periods have been chosen to be consecutive which should minimise these effects leading to a meaningful comparison.

Figure 14 shows that the globally averaged standard deviation of background departures is significantly reduced in v724 compared to v620 for the RFI screened sample (darker bars). Due to the different periods for the v724 and v620 data there is also a reduction in the standard deviation of background departures in the data sample without RFI screening, indicating slightly lower levels of RFI during the August period of the v724 data. However, the difference in the samples with the RFI screening is larger than without, particularly for V polarisation, which indicates that the RFI screening does appear to be improved in v724. For example, for V polarisation the global standard deviation reduces by 6.1% from 21.2K to 19.9K for all data; and by 14.6% from 15.8K to 13.5K for the RFI screened data. The number of observations passing the screening is also reduced in v724 compared to v620 (not shown, but indicated by figures 1 to 3).

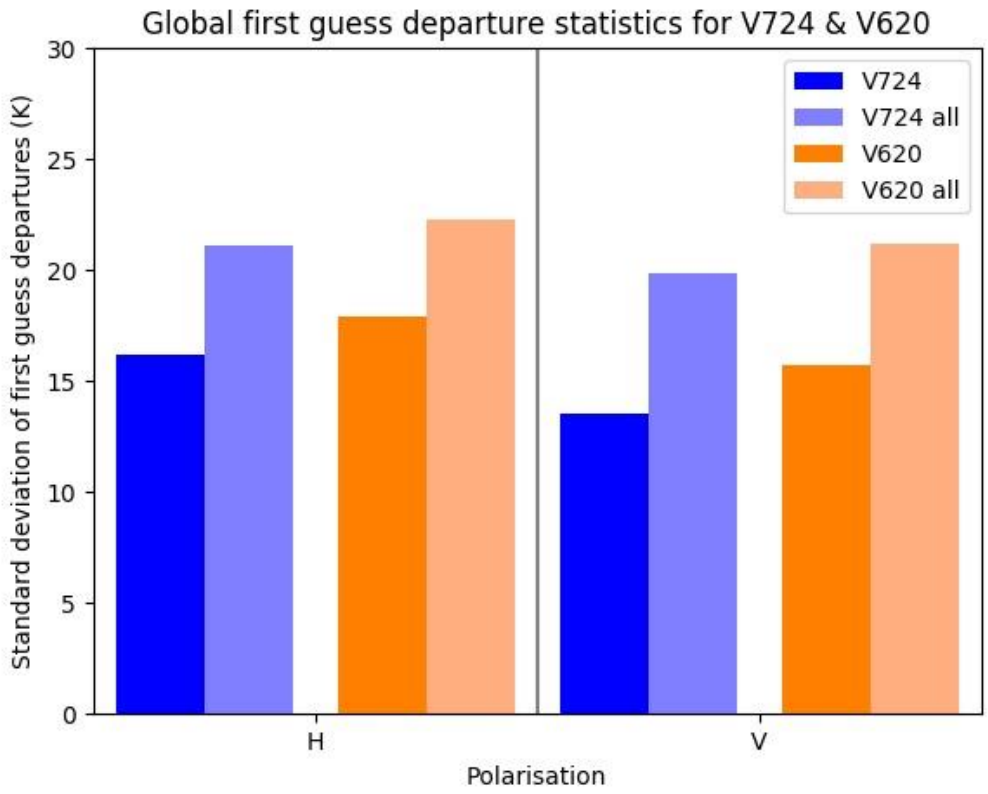

Figure 14: Globally averaged standard deviation of SMOS background departures for H polarisation (left) and V polarisation (right); v724 (blue bars) and v620 (orange bars). The lighter coloured bars are for all data without RFI screening, the darker bars are with RFI screening applied. Statistics are accumulated between 1st July 2021 and 31st August 2021.

Figure 15 shows that, over land, the largest differences in the standard deviation of background departures are concentrated over areas we expect to be affected by RFI such as Eastern Asia, the Middle East and South-Eastern Europe. This provides further evidence that the RFI screening is enhanced in v724. It also shows smaller reductions in the standard deviation of background departures in areas not expected to be affected by RFI such as Australia and the Americas which suggest that the v724 product also has lower noise than v620 product. There are some small areas of slight increases in the standard

deviation of background departures, e.g. over Northern Siberia, but the vast majority of regions show a reduction and therefore a better agreement between the observations and the simulated Tbs.

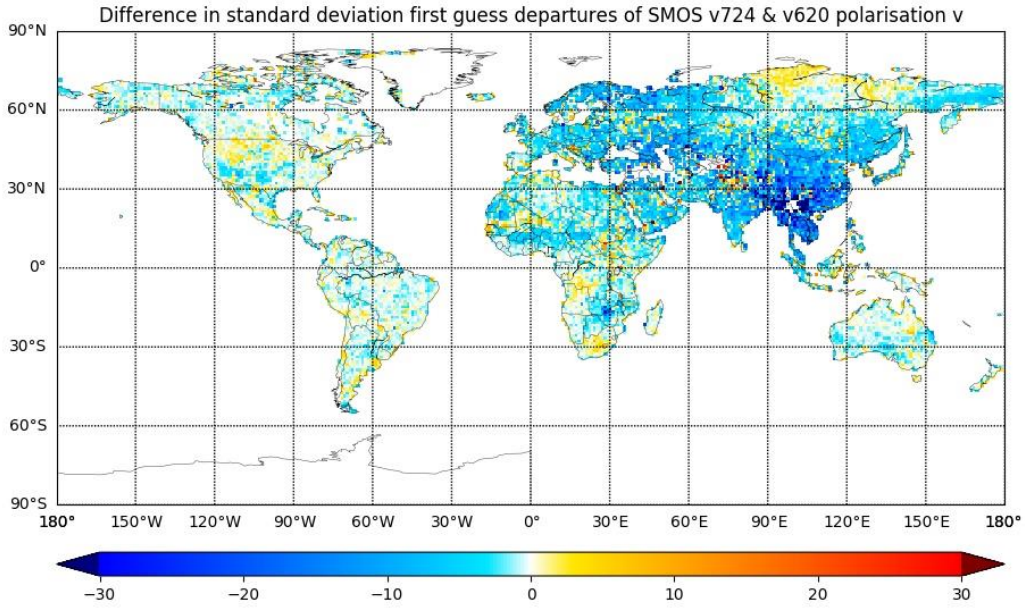

Figure 15: Difference in gridded standard deviation of SMOS background departures for V polarisation between v724 and v620. Statistics are calculated between 1st July and 31st August 2021

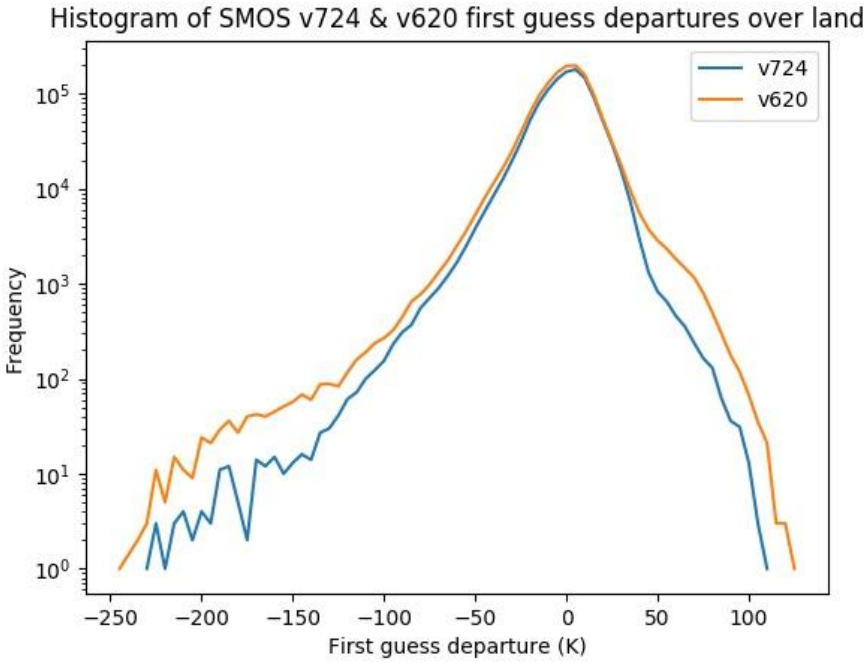

Figure 16: Histogram of the SMOS background departure distribution for H polarisation; for v724 (blue) and v620 (orange). The data are from between 1st July and 31st August 2021

Figure 16 shows that the background departure distribution has significantly reduced tails for the v724 Tbs compared to the v620 Tbs. This is another indication that the observations in gross disagreement with the simulations are being screened out better in v724 than in v620.

Overall, it appears that the v724 SMOS L1 Tbs have significantly improved RFI screening information when compared to the v620 product. There are also indications that the level of noise in the v724 observations is lower than for v620 in areas not affected by RFI. The combined effect is that the v724 observations agree better with the simulated ECMWF model values so the move to the v724 product represents an improvement over the v620 product.

4. Future enhancements to the monitoring system

4.1. Bias correction

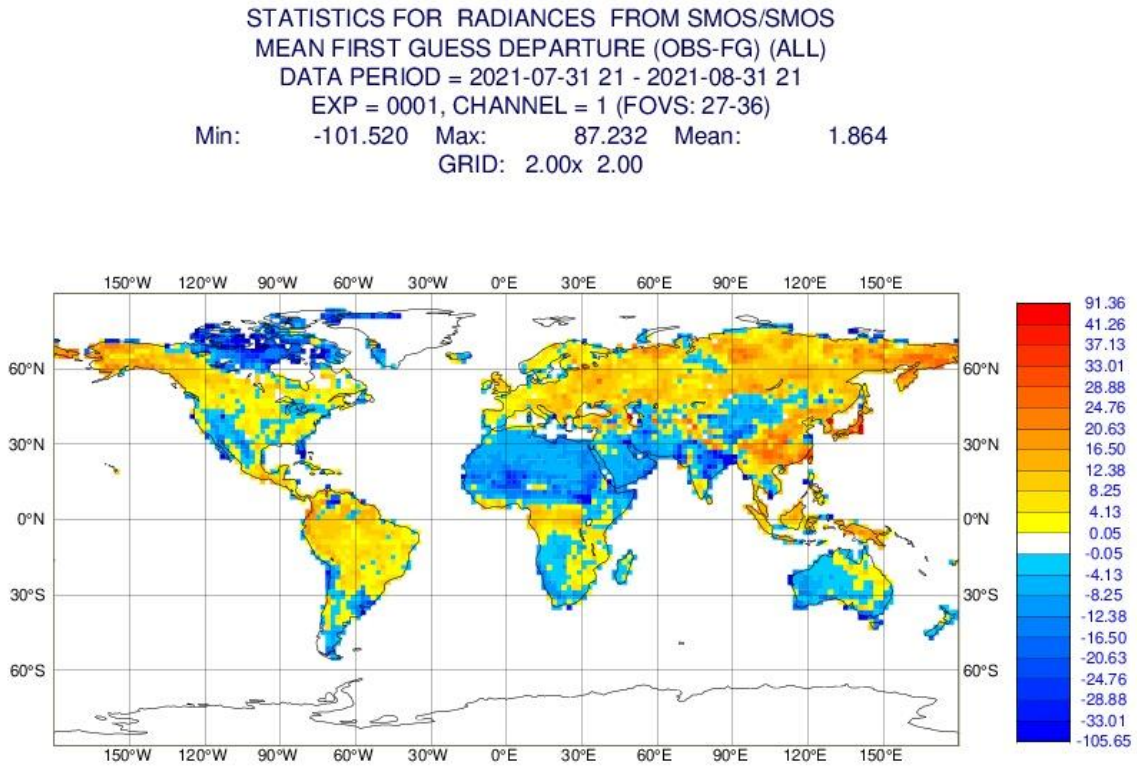

Figure 17: Map plot showing the mean of SMOS background departures over land at 30° incidence angle, H polarisation covering 1st August to 31st August 2021

Figure 17 shows the global distribution of biases between the observations and the model equivalent values without any bias correction applied. There are positive biases over Europe, most of Asia and South America and negative biases over most of Africa, Australia and Northern Canada. Generally the negative biases seem to be located in drier regions indicating the model soil moisture is too dry compared to the observations.

In most data assimilation methods the observations and model are assumed to be unbiased relative to one another. Therefore, to enable the assimilation of the SMOS observations a bias correction procedure will need to be developed. In a monitoring context, de Rosnay et al. (2020) showed that applying a bias correction to SMOS L1 Tbs significantly improves the background departure statistics, which will enable the monitoring to be even more sensitive to smaller changes and shifts in the data quality.

4.2. RFI screening

As shown in section 2 and 3.2 of this report the latest RFI screening has been significantly improved but remains sub-optimal and misses screening out many SMOS observations which are clearly affected by RFI. ECMWF has been part of the ESA RFI4EO project led by Zenithal Blue Technologies aimed at using various statistical and pattern recognition algorithms (ground RFI detection system - GRDS) to improve the RFI screening (Oliva et al., 2021). Preliminary results using a month of SMOS data indicate that the new system demonstrates significant improvements over the v620 screening, for example see figure 18, where hot spots over Northern India and the middle East are almost completely removed when the GRDS screening is applied.

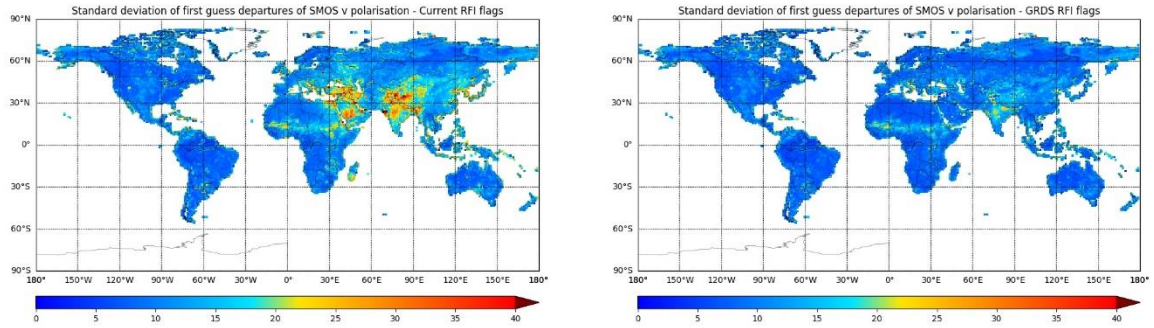

Figure 18: Gridded maps of standard deviation of SMOS background departures at V polarisation with the operational v620 RFI screening (left) and new GRDS-based screening (right). The sample of data for both plots is the same and comes from between 1st July 2019 and 31st July 2019

Given these results, and pending results of comparisons with the v724 screening, it is proposed to implement the newly developed GRDS for SMOS to further improve the RFI screening of operational products.

4.3. Improved monitoring over ocean

There is ongoing work at ECMWF to improve the sea-ice and coastal screening in other MW radiance observations which could be applied to SMOS data in the future. In particular, the use of FASTEM (Liu et al., 2011) as part of the RTTOV (Saunders et al., 2018) radiative transfer model to calculate surface emissivities over ocean could be used to produce more realistic and accurate simulated Tbs for SMOS over ocean. In coastal areas a weighted average of the FASTEM/RTTOV simulated Tb and the CMEM simulated Tb using the fraction land-ocean mask information could be used. This has the potential to significantly improve the quality of the background departures in coastal regions and could lead to the relaxation of the coastal screening documented in section 3.1.

4.4. Multi-year monitoring

To expand on the assessment of the v724 reprocessed SMOS L1 Tbs it is also planned to develop multi-year monitoring for the entire SMOS lifetime (2010-present) (de Rosnay and Weston, 2019). This activity, in context of the ESA SMOS-E project, has already begun with the acquisition of 11 years of SMOS data and monitoring experiments will be run over the next year. The aim is to assess trends over the 11+ year period by comparing the observations to the ERA5 reanalysis which will provide a stable and consistent baseline. The SMOS multi-year reprocessed data monitoring will be complementary to the current operational monitoring.

5. Comparisons to SMAP

As part of the operational change on 11th May 2021 the monitoring of the NASA Soil Moisture Active Passive (SMAP) instrument was also added to the operational system, using the same framework as the SMOS monitoring. SMAP was launched in 2015 and the instrument measures at L-band (1.41GHz) the same frequency as SMOS and therefore comparisons between the monitoring statistics for SMOS and SMAP are very relevant for unpicking observation and model issues in the background departures.

The comparisons presented in section 5.1 were made with data from August 2021 with the new v724 SMOS L1 Tbs and most up-to-date SMAP Tbs in the operational system. The SMOS observations used in the comparison are limited to those with incidence angles between 39.5° and 40.5° which best match the 40° incidence angles of the SMAP observations. Also, the operational screening including the most up-to-date RFI screening is applied to the SMOS data. By contrast, SMAP has onboard RFI screening which is applied to the data before it arrives at ECMWF. CMEM with the same settings is used as the observation operator or both the SMOS and SMAP observations.

5.1. August 2021 comparison

Figure 19 shows that the standard deviation of background departures is slightly larger for SMAP than for SMOS for H polarisation but significantly smaller for V polarisation. For both polarisations the SMAP mean background departures are more negatively biased with the magnitude of bias larger than for SMOS. Although there are differences the statistics are largely comparable which is encouraging given both instruments measure at the same frequency and are sensitive to the same geophysical signals.

Figure 20 shows that for H polarisation the gridded standard deviation of background departures are significantly smaller for SMAP than they are for SMOS with the largest differences in Asia, the middle East and South-Eastern Europe, all areas where there are significant RFI sources. This indicates that the onboard screening for SMAP is still doing a better job than the v724 SMOS screening. In addition, over areas not affected by RFI, the SMAP standard deviation of background departures are also smaller than for SMOS. This indicates that SMAP has lower instrument noise than SMOS which is expected because the SMOS instrument was designed to reduce the noise by averaging over different incidence angles. In this analysis only a small range of SMOS incidence angles are used so there is no reduction in noise from the use of multiple incidence angles.

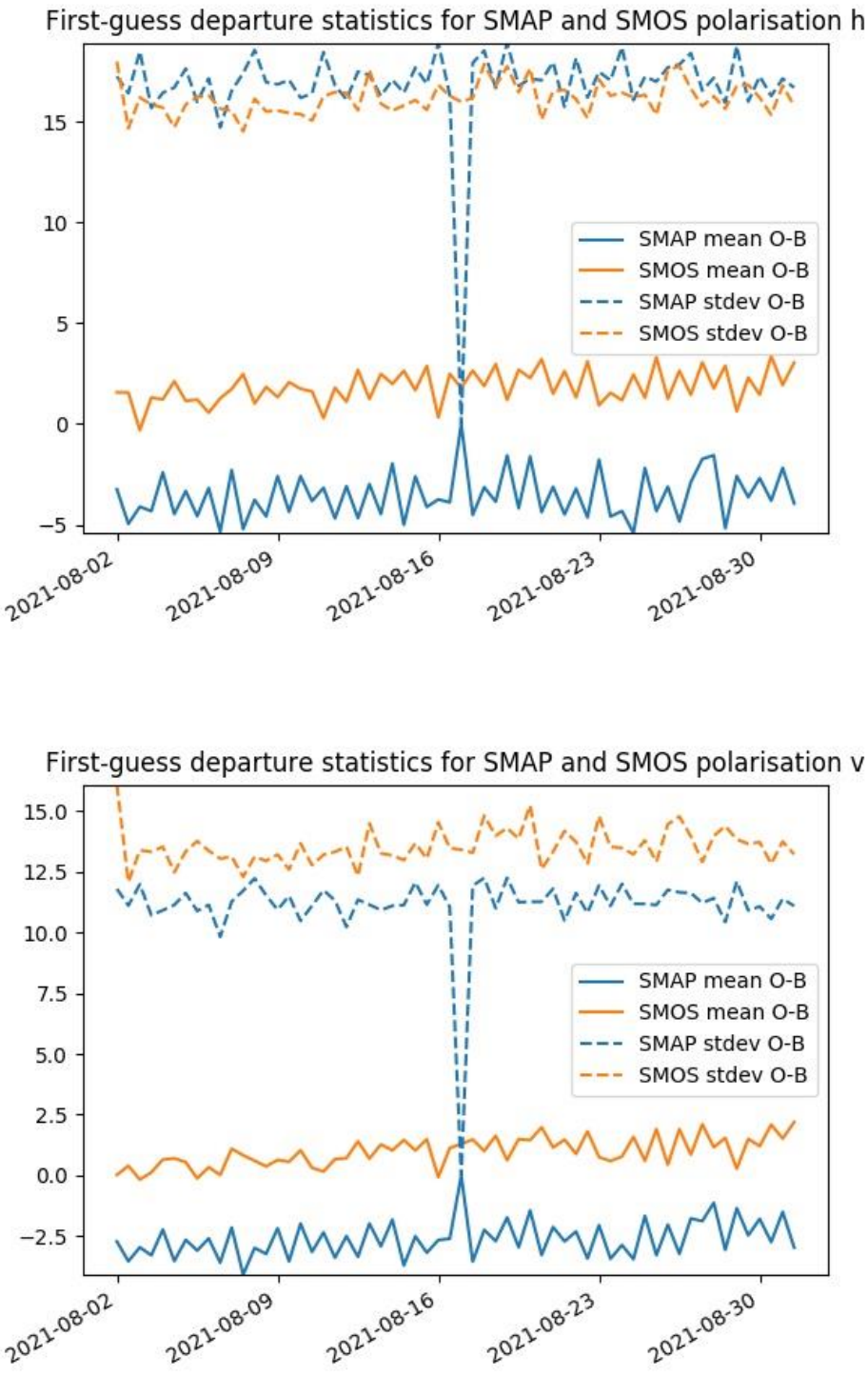

Figure 19: Time series of mean (solid lines) and standard deviation (dashed lines) of background departures for SMAP (blue) and SMOS (orange) for H polarisation (upper) and V polarisation (lower) between 2nd August and 31st August 2021

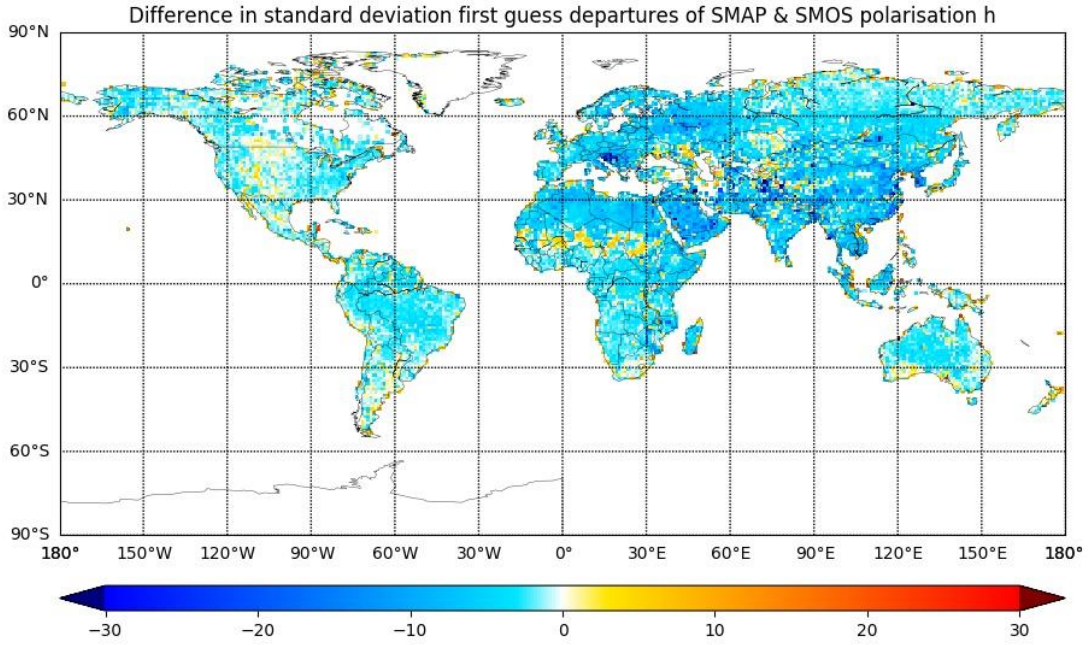

Figure 20: Difference in gridded standard deviation of background departures for H polarisation between SMAP and SMOS. Statistics are calculated between 2nd August and 31st August 2021

It would appear that figure 20 and the upper panel of figure 19 contradict each other, with figure 19 suggesting SMAP has larger standard deviation of background departures than SMOS and figure 20 suggesting the opposite. It is worth considering that the global standard deviation of background departures combines two forms of variability: temporal variability; and spatial variability. In the gridded map of figure 20 the spatial variability is removed because the statistics are accumulated grid point by grid point but the temporal variability remains. This suggests that the spatial variability in the background departures is larger for SMAP than for SMOS. This can be investigated by looking at the regional biases in figure 21.

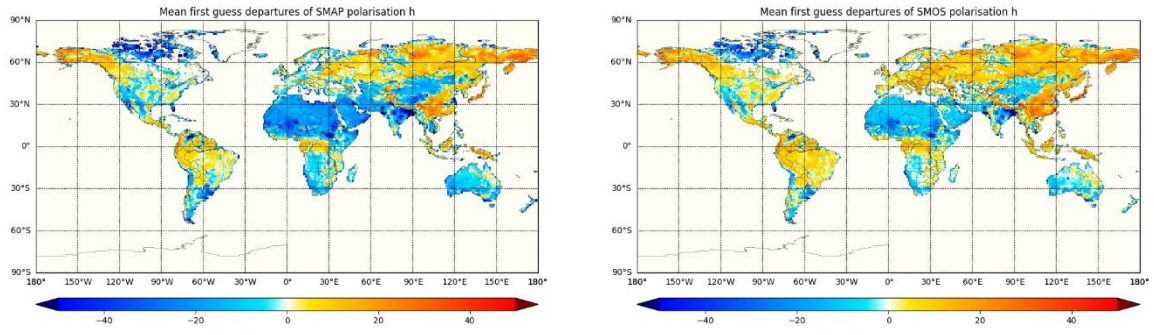

Figure 21: Gridded maps of mean background departures at H polarisation for SMAP (left) and SMOS (right). The sample of data for both plots is the same and comes from between 2nd August and 31st August 2021

The global bias patterns in figure 21 are similar but it can be seen that there are generally darker colours (both positive and negative) for SMAP than for SMOS indicating that the regional biases are larger for SMAP and hence that the spatial variability is also larger. This is borne out when taking the standard deviation of these gridded mean background departure maps with 8.0K for SMAP compared to 6.5K for SMOS. For V polarisation these values are much more similar for SMOS and SMAP which means that SMAP has consistently smaller standard deviation of background departures both globally and on the gridded maps (not shown).

Overall, the temporal standard deviation of background departures are smaller for SMAP than for SMOS, which is due to a combination of the effective onboard RFI screening for SMAP and lower instrument noise. However, the SMAP departures are more negatively biased with a larger magnitude of the global bias and larger variability in the regional biases than for SMOS. The SMAP and SMOS monitoring at ECMWF will continue in the future and further comparisons will be made to investigate the differences and similarities between the performance of the two instruments.

Appendix A: Quality control procedures (as implemented from 11th May 2021 onwards)

Data quality information is supplied with each observation in the NRT BUFR files. A series of bits in the SMOS BUFR flag table (de Rosnay et al, 2021) are set to indicate any problems with the associated data. Table 3 shows a summary of these bits and the meaning of each one.

At ECMWF, before the monitoring runs, a pre-screening program is run to remove observations which are known to contain anomalous data or cannot be handled successfully by the monitoring system. Currently, if bit number 3 of the SMOS information flags in the SMOS input BUFR files is set then this indicates that the observation is in the border between the exclusive alias-free zone and the extended alias-free zone and any observations with this bit set are not processed any further. In addition, bit number 7 indicates that data has been affected by solar reflection and any observations with this bit set are not processed any further. Any observations which have any of bit numbers 1, 4 or 9 set are affected by RFI and, although these are processed by the monitoring system, there are a set of monitoring plots which only plot data without any of these bits being set i.e. those observations not affected by RFI.

After the pre-screening the remaining SMOS observations are read into the IFS and further screening procedures are undertaken to avoid areas where the observations cannot be accurately modelled by CMEM, for example over snow-covered surfaces. These are summarised in table 4. In addition to the checks in table 4 each observation location is classified as land if the model land-sea mask value in the collocated gridpoint is greater than 0.95 and sea if the land-sea mask value is less than 0.01. The procedures in table 4 are performed for observations over both land and sea but it would be possible to implement different quality control procedures depending on whether the observation is over land or sea if deemed necessary.

Bit number	Meaning
1	**Pixel is affected by RFI effects as identified in the AUX_RFILST or it has exceeded the BT thresholds**
2	Pixel is located in the hexagonal alias directions centred on a Sun alias (if Sun is not removed, measurement may be degraded in these directions)
3	**Pixel is close to the border delimiting the Extended Alias free zone or to the unit circle replicas borders.**
4	**Measurement is affected by the tails of a point source RFI as identified in the AUX RFI list (tail width is dependent on the RFI expected BT, from each snapshot measurements, corresponding to 0.16 of the radius of the RFI circle flagged)**
5	Pixel is inside the exclusive zone of Alias free.
6	Pixel is located in a zone where a Moon alias was reconstructed
7	**Pixel is located in a zone where Sun reflection has been detected**
8	Pixel is located in a zone where a Sun alias was reconstructed
9	**Measurement is affected by RFI effects as identified in the AUX_RFI list whose contribution generates a contamination in Brightness Temperature above 30K in the corresponding polarization (v724 since 2nd August 2021)** **Measurement is affected by RFI effects in the corresponding polarisation as identified in the long trend analysis of telemetry data (NIR and System Temperatures) (v620 until 1st August 2021)**
10	Scene has not been combined with an adjacent scene in opposite polarisation during image reconstruction
11	Direct Moon correction has been performed during image reconstruction of this pixel
12	Reflected Sun correction has been performed during image reconstruction of this pixel
13	Direct Sun correction has been performed during image reconstruction of this pixel
All 14	Missing value

Table 3: SMOS information flags from the flag table (code 025144) as part of the SMOS NRT product specification. Options in bold are currently used for SMOS brightness temperature data quality control for operational monitoring at ECMWF.

Screening reason	Threshold for rejection
Extreme values	Measured Tb less than 50K or greater than 340K
Snow	Model snow depth greater than 1cm
Frozen surfaces	Model 2 metre temperature less than 273K
Sea ice	Model sea ice concentration greater than 1%
Coasts	Model land-sea mask values between 0.01 and 0.95

Table 4: Quality control applied to SMOS observations within the IFS

Figure 22 shows the geographical distribution of the surface type and quality control applied. As expected most observations at high latitudes are screened out by the snow, frozen surface and sea ice checks. There are RFI detections over the middle East, Eastern Europe and parts of Asia. Very few observations are screened out by the simple extreme value check. Around all of the coasts, inland lakes and small islands observations are screened out by the coast check.

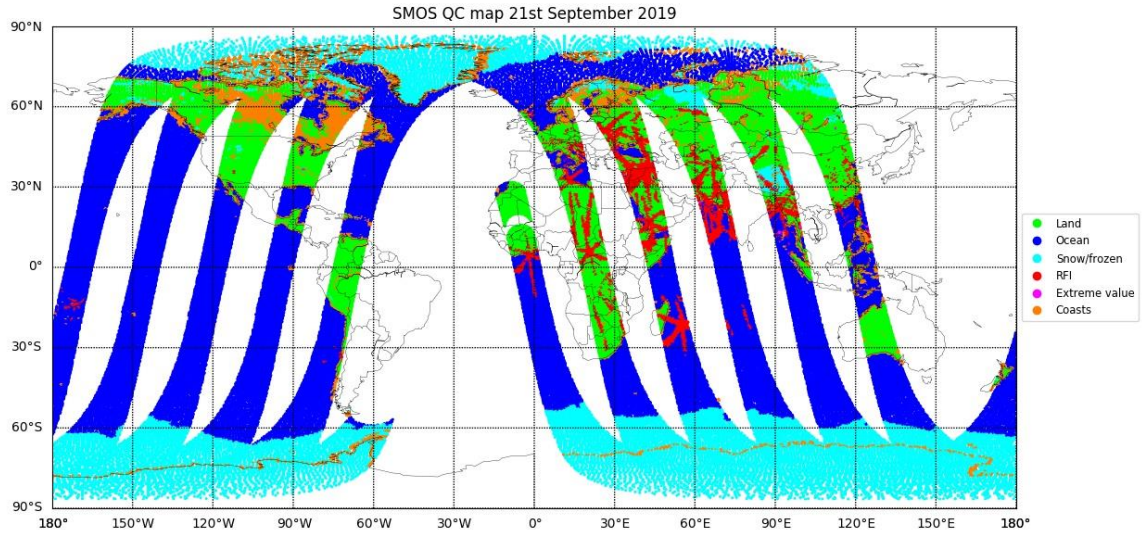

Figure 22: Map showing SMOS observations classified by surface type (land: green; sea: blue) and quality control rejection reason (extreme value: magenta; snow, frozen ground or sea ice: cyan; RFI: red; coasts: orange) for data between 09:00 and 21:00 UTC on 21st September 2019

Figure 23 provides a breakdown of typical numbers of observations during a 12 hour period which are classified as land or sea and also the numbers of observations screened out by the checks detailed in table 4. The check which screens out the most observations is the snow/frozen surfaces check and this number increases further in the Northern hemisphere winter when snow covers much of Canada and Russia. The coastal screening accounts for the next most, followed by RFI and finally the extreme value check accounts for the least.

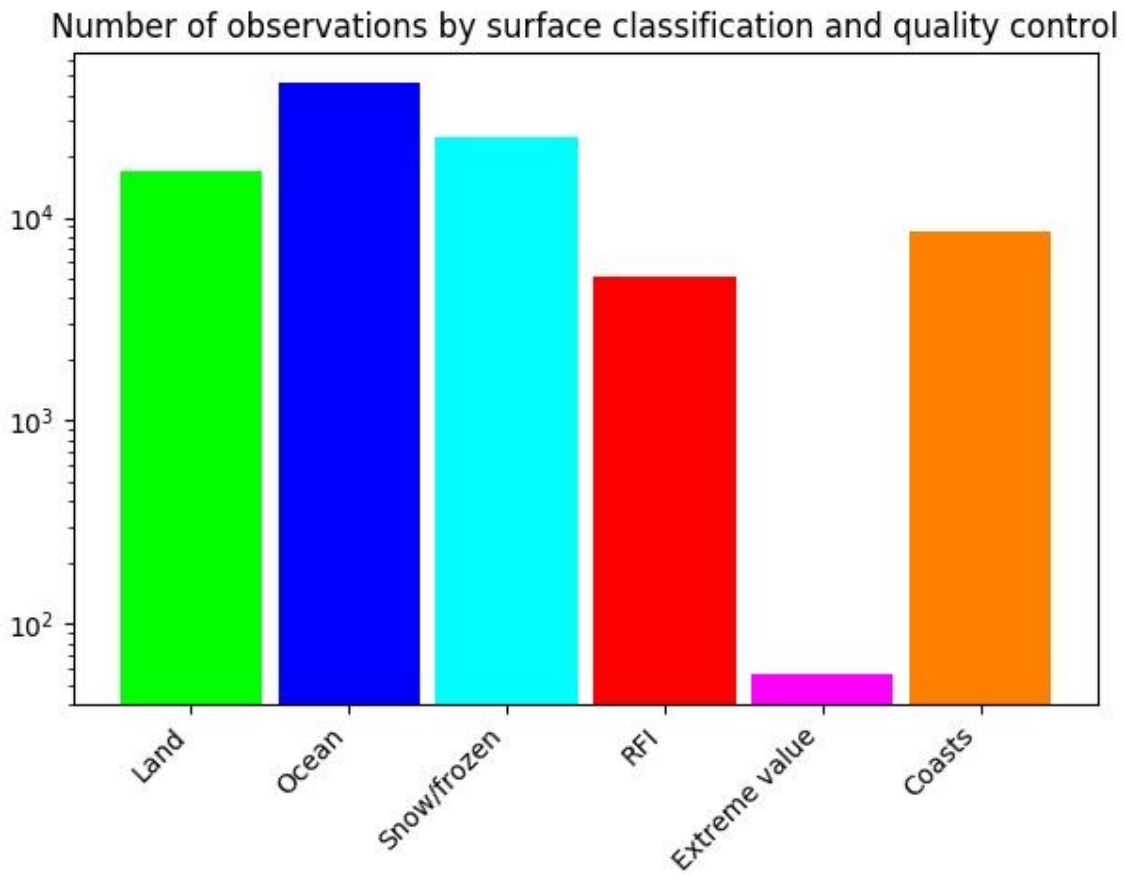

Figure 23: Bar chart showing the breakdown of number of SMOS observations classified by surface and quality control check triggered for data between 09:00 and 21:00 UTC on 21st September 2019. Note the logarithmic scale

References

de Rosnay, P., M. Dragosavac, M. Drusch, A. Gutiérrez, M. Rodríguez López, N. Wright, J. Muñoz Sabater, Raffaele Crapolicchio: SMOS NRT BUFR specification, 25/05/2021. SMOS_NRT_BUFR_ECMWF_v1.9 (esa.int)

de Rosnay P. and P. Weston: SMOS long-term assessment based on re-analyses: strategy and work plan", ESA contract report. ESA SMOS-E contract 4000125399/18/I-BG, December 2019

de Rosnay, P., J. Muñoz-Sabater, C. Albergel, L. Isaksen, S. English, M. Drusch, J.-P. Wigneron: SMOS brightness temperature forward modelling and long term monitoring at ECMWF. Remote Sens. Environ., 237 (2020): 111424. https://doi.org/10.1016/j.rse.2019.111424

Liu, Q., Weng, F., and English, S.: An improved fast microwave water emissivity model, IEEE, T. Geosci. Remote, 49, 1238–1250, 2011.

Oliva, R., A. Martellucci, E. Daganzo-Eusebio, F. Jorge, Y. Soldo, S. English, P. de Rosnay, P. Weston, J. Barbosa, I. Nestoras "Results from the ground RFI detection system for passive microwave Earth observation data" IGARSS 2021

Saunders, R., Hocking, J., Turner, E., Rayer, P., Rundle, D., Brunel, P., Vidot, J., Roquet, P., Matricardi, M., Geer, A., Bormann, N., and Lupu, C.: An update on the RTTOV fast radiative transfer model (currently at version 12), Geosci. Model Dev., 11, 2717–2737, https://doi.org/10.5194/gmd-11-2717-2018, 2018.

Weston, P., P. de Rosnay: Quality control plan for brightness temperature monitoring. ESA contract report. SMOS ESL contract 4000130567/20/I-BG, July 2020

Weston, P., P. de Rosnay: Annual SMOS brightness temperature monitoring report - 2019/20. ESA contract report. SMOS ESL contract 4000130567/20/I-BG, January 2021a

Weston, P., de Rosnay, P. SMOS brightness temperature monitoring quality control review and enhancements. *Remote Sens.* 2021b. in press, https://doi.org/10.3390/rs13204081.